

Electromagnetic corrections in hadronic tau decays

A. Miranda

Institut de Física d'Altes Energies (IFAE) and The Barcelona Institute of Science and Technology, Campus UAB, 08193 Bellaterra (Barcelona), Spain.

Received 15 May 2023; accepted 13 July 2023

We revisit the isospin-breaking and electromagnetic corrections of some hadronic tau decays, which can also be employed to extract the Cabibbo-Kobayashi-Maskawa (CKM) matrix element V_{us} . We extend former analyses by Antonelli *et al.* working with ChPT with resonances. We find that going beyond the Low approximation, these corrections play an important role between the $\pi^- K^0$ and $K^- \pi^0$ modes. The $K^- K^0$ channel is also discussed.

Keywords: Radiative corrections; effective field theory; semileptonic decays.

DOI: <https://doi.org/10.31349/SuplRevMexFis.4.021115>

1. Introduction

Semileptonic tau decays are a valuable tool for studying QCD hadronization at low energies [1,2], as the τ lepton is the only known lepton that is heavy enough to decay into hadrons. With the high-precision measurements achieved in recent years [3–10], one- and two-meson decays of tau leptons have become increasingly useful for testing new physics scenarios [11–23]. To this end, it is crucial to account for radiative corrections in the theoretical predictions.

One-meson transitions $\tau^- \rightarrow P^- \nu_\tau$ ($P = K, \pi$) have been extensively studied [20, 21, 24–26] and are well-understood thanks to the precise determination of the pion and kaon decay constants obtained by lattice QCD collaborations [27]. Two-meson transitions, on the other hand, have been examined in detail mainly for the $\pi^- \pi^0$ decay mode [28–31], which is used in the dispersive evaluation of the leading-order hadronic vacuum polarization contribution to the muon $g - 2$ [28, 29, 32]. The $(K\pi)^-$ decay mode has also been investigated [33, 34] and can be employed to extract the Cabibbo-Kobayashi-Maskawa matrix.

This paper is organized as follows. In Sec. 1, we discuss the amplitude for the $\tau^- \rightarrow P_1^- P_2^0 \nu_\tau \gamma$ decays. Some observables for these decays are presented in Sec. 2. In Sec. 3, we evaluate the radiative corrections. Finally, our conclusions are presented in Sec. 4.

2. Amplitude for $\tau^- \rightarrow P_1^- P_2^0 \nu_\tau \gamma$

The most general amplitude that describes the $\tau^-(P) \rightarrow P_1^-(p_-) P_2^0(p_0) \nu_\tau(q) \gamma(k)$ decays reads

$$\mathcal{M} = \frac{e G_F V_{ud}^*}{\sqrt{2}} \epsilon_\mu^* \left[(V^{\mu\nu} - A^{\mu\nu}) \bar{u}(q) \gamma_\nu (1 - \gamma^5) u(P) + \frac{H_\nu(p_-, p_0)}{k^2 - 2k \cdot P} \bar{u}(q) \gamma^\nu (1 - \gamma^5) (m_\tau + \not{P} - \not{k}) \gamma^\mu u(P) \right], \quad (1)$$

where $P_{1,2}$ refers to a pseudoscalar meson, and

$$H^\nu(p_-, p_0) = C_V F_+(t) Q^\nu + C_S \frac{\Delta_{-0}}{t} q^\nu F_0(t), \quad (2)$$

with $t = q^2$, $Q^\nu = (p_- - p_0)^\nu - (\Delta_{-0}/t) q^\nu$, $q^n u = (p_- + p_0)^\nu$, $\Delta_{12} = m_1^2 - m_2^2$ and $C_{V,S}$ is a Clebsch-Gordan (CG) coefficient. The vector and axial terms in the first line in Eq. (1) can be split in two parts, structure-independent (SI) and structure-dependent (SD), in compliance with the Low and Burnett-Kroll theorems [35, 36].

The structure-independent term is given by [29, 37]

$$V_{\text{SI}}^{\mu\nu} = \frac{H^\nu(p_- + k, p_0)(2p_- + k)^\mu}{2k \cdot p_- + k^2} + \left\{ -C_V F_+(t') - \frac{\Delta_{-0}}{t'} [C_S F_0(t') - C_V F_+(t')] \right\} g^{\mu\nu} - C_V \frac{F_+(t') - F_+(t)}{k \cdot (p_- + p_0)} Q^\nu q^\mu + \frac{\Delta_{-0}}{tt'} \left\{ 2 [C_S F_0(t') - C_V F_+(t')] - \frac{C_S t'}{k \cdot (p_- + p_0)} [F_0(t') - F_0(t)] \right\} q^\mu q^\nu, \quad (3)$$

where $t' = (P - q)^2$.

Hereafter, we will discuss the strange-changing and -conserving modes *i.e.*, $K^- \pi^0$, $\bar{K}^0 \pi^-$ and $K^- K^0$, respectively. The usual definition of $H_{K\pi}^\nu$ [15] is recovered by substituting $p_- \rightarrow p_K$, $p_0 \rightarrow p_\pi$ and $\Delta_{-0} \rightarrow \Delta_{K\pi}$ for $K^- \pi^0$, and $p_- \rightarrow p_\pi$, $p_0 \rightarrow p_K$, $C_{V,S} \rightarrow -C_{V,S}$ and $\Delta_{-0} \rightarrow -\Delta_{K\pi}$ for $\bar{K}^0 \pi^-$. The CG coefficients for these modes are $C_{V,S}^{K\pi, \bar{K}\pi, KK} = \{1/\sqrt{2}, 1, -1\}$.

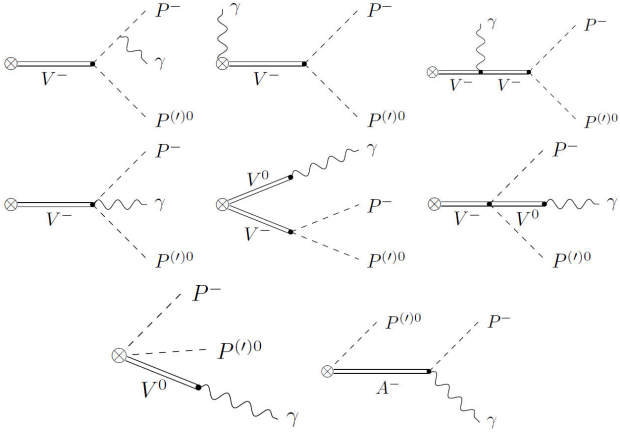


FIGURE 1. Vector and axial-vector meson exchange diagrams contributing to the $\tau^- \rightarrow P_1^- P_2^0 \nu_\tau \gamma$ decays at $\mathcal{O}(p^4)$. V^0 stands for the ρ^0 , ω and ϕ resonances, $V^- = K^{*-}$ for the $K\pi$ modes and $V^- = \rho^-$ for the $K^- K^0$ one, $A^- = K_1^-$ in $K^- K^0$ and $K^- \pi^0$, and $A^- = a_1^-$ in $\pi^- \bar{K}^0$.

The structure-dependent (SD) contribution is parameterized by four vector and four axial-vector form factors. These terms can be written as

$$\begin{aligned} V_{SD}^{\mu\nu} &= v_1(k \cdot p_- g^{\mu\nu} - k^\nu p_-^\mu) + v_2(k \cdot p_0 g^{\mu\nu} - k^\nu p_0^\mu) \\ &+ v_3(k \cdot p_0 p_-^\mu - k \cdot p_- p_0^\mu) p_-^\nu \\ &+ v_4(k \cdot p_0 p_-^\mu - k \cdot p_- p_0^\mu) (p_- + p_0 + k)^\nu, \end{aligned} \quad (4)$$

and

$$\begin{aligned} A_{\mu\nu}^{SD} &= i a_1 \epsilon_{\mu\nu\rho\sigma} (p_0 - p_-)^\rho k^\sigma + i a_2 (P - q)_\nu \epsilon_{\mu\rho\sigma\tau} k^\rho p_-^\sigma p_0^\tau \\ &+ i a_3 \epsilon_{\mu\nu\rho\sigma} k^\rho (P - q)^\sigma + i a_4 (p_0 + k)_\nu \epsilon_{\mu\lambda\rho\sigma} k^\lambda p_-^\rho p_0^\sigma, \end{aligned} \quad (5)$$

where p_- and p_0 are the momentum of the charged and neutral meson, respectively.

The SD part is evaluated using ChPT with resonances up to $\mathcal{O}(p^4)$ [38, 39]. The diagrams contributing to the vector form factors in Eq. (4) are shown in Fig. 1. The axial form

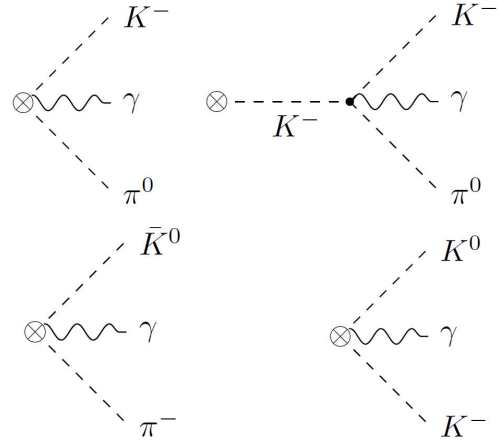


FIGURE 2. Axial contributions to the $\tau^- \rightarrow P_1^- P_2^0 \nu_\tau \gamma$ decays at $\mathcal{O}(p^4)$.

factors are only saturated by the Wess-Zumino-Witten functional [40,41] since the resonance exchange contribution start at $\mathcal{O}(p^6)$. The diagrams that contribute to the axial form factors are depicted in Fig. 2, as we can see, two diagrams contribute to the $K^- \pi^0$ decay mode while only one contributes to the $\bar{K} \pi^-$ and $K^- K^0$ channels. The full expressions for the v_i and a_i form factors can be found in Ref. [42].

3. Decay rate and spectrum

The differential rate for these decays in the τ rest frame reads

$$d\Gamma = \frac{(2\pi)^4}{4m_\tau} \sum_{\text{spin}} |\overline{\mathcal{M}}|^2 d\Phi_4, \quad (6)$$

where $d\Phi_4$ is the associated 4-body phase space, and $|\overline{\mathcal{M}}|^2$ is the unpolarized spin-averaged squared amplitudeⁱ.

The branching ratios are depicted in Fig. 3 and summarized in Table I as a function of E_γ^{cut} . The red dashed line represents the branching ratio using the amplitude in the Low

TABLE I. Branching ratios $\text{Br}(\tau^- \rightarrow K^- \pi^0 \nu_\tau \gamma)$ for different values of E_γ^{cut} . The third column corresponds to the complete bremsstrahlung, and the fourth to the $\mathcal{O}(p^4)$ contributions in $\text{R}\chi\text{T}$.

	E_γ^{cut}	Low	SI	$\text{R}\chi\text{T}$
$\mathcal{B}_{K^- \pi^0}$	100 MeV	3.4×10^{-6}	3.0×10^{-6}	$3.8(3) \times 10^{-6}$
	300 MeV	6.2×10^{-7}	3.4×10^{-7}	$9.4(3.1) \times 10^{-7}$
	500 MeV	7.4×10^{-8}	3.5×10^{-8}	$3.3(1.8) \times 10^{-7}$
$\mathcal{B}_{\bar{K}^0 \pi^-}$	100 MeV	2.6×10^{-5}	1.4×10^{-5}	$1.6(0) \times 10^{-5}$
	300 MeV	6.2×10^{-6}	1.1×10^{-6}	$1.9(2) \times 10^{-6}$
	500 MeV	1.0×10^{-6}	7.1×10^{-8}	$2.4(4) \times 10^{-7}$
$\mathcal{B}_{K^- K^0}$	100 MeV	5.3×10^{-7}	3.7×10^{-7}	$9.4(2.6) \times 10^{-7}$
	300 MeV	4.8×10^{-8}	1.9×10^{-8}	$3.1(1.4) \times 10^{-7}$
	500 MeV	3.7×10^{-10}	3.0×10^{-10}	$2.9(1.8) \times 10^{-8}$

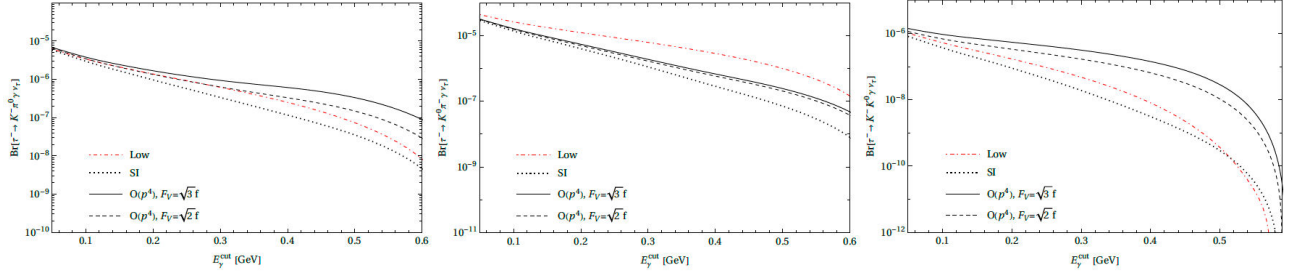


FIGURE 3. Branching ratio predictions for the $\tau^- \rightarrow K^- \pi^0 \nu_\tau \gamma$ (left), the $\tau^- \rightarrow \bar{K}^0 \pi^- \nu_\tau \gamma$ (center) and the $\tau^- \rightarrow K^- K^0 \nu_\tau \gamma$ (right) decays as a function of E_γ^{cut} . The solid and dashed line represent the $\mathcal{O}(p^4)$ corrections using $F_V = \sqrt{3}F$ and $F_V = \sqrt{2}F$, respectively. The dotted line represents the bremsstrahlung contribution (SI). The red one corresponds to the Low approximation.

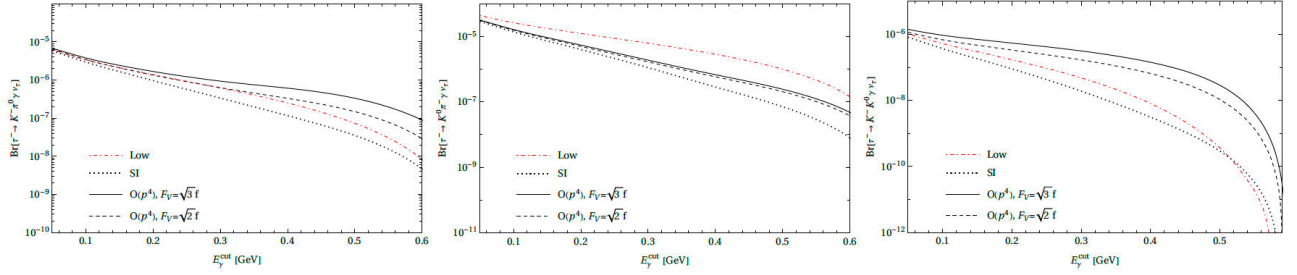


FIGURE 4. The $K^- \pi^0$ (left), $\bar{K}^0 \pi^-$ (center) and $K^- K^0$ (right) hadronic invariant mass distributions for $E_\gamma^{\text{cut}} \geq 300$ MeV.

limit, while the dotted one shows the SI prediction with $v_i = a_i = 0$. The solid and dashed lines correspond to the SD prediction of the branching ratios using $F_V = \sqrt{3}F$, $G_V = F/\sqrt{3}$ and $F_A = \sqrt{2}F$ [43–46], and $F_V = \sqrt{2}F$, $G_V = F/\sqrt{2}$ and $F_A = F$ [39], respectivelyⁱⁱ. For simplicity, we refer as $3F$ and $2F$ to these two approaches. In the last column in Table I, we use the $3F$ result as the central value and the difference with respect to $2F$ as a symmetric error. As we can see, the Low's approximation describe very well this transitions for $E_\gamma^{\text{cut}} \leq 100$ MeV.

The corresponding hadronic invariant mass distributions for $E_\gamma^{\text{cut}} \geq 300$ MeV are shown in Fig. 4. The $\bar{K}^0 \pi^-$ distribution shows a large difference between the Low prediction and all the other approaches which is not evident for the $K^- \pi^0$ case. This difference can be attributed to a sign differ-

ence between the $\bar{K}^0 \pi^-$ and $K^- \pi^0$ modes in the term proportional to $g^{\mu\nu}$ in Eq. (3). This term is absent in the Low's approximation since it is a properly $\mathcal{O}(k^0)$ contribution, and as we mention above, this approximation is not sufficient to describe these decays for energies above 100 MeV. On the other hand, the $K^- K^0$ invariant mass distribution is more sensitive to SD contributions. All these features make these decays an excellent probe for testing SD effects. The photon energy distribution and the SI decay spectrum for different E_γ^{cut} are also studied in Ref. [42].

4. Radiative Corrections

The overall differential decay width, which includes the contributions from virtual and real photons, is given by

$$\begin{aligned} \frac{d\Gamma}{dt} \Big|_{PP(\gamma)} &= \frac{G_F^2 |V_{uD}F_+(0)|^2 S_{\text{EW}} m_\tau^3}{768\pi^3 t^3} \left(1 - \frac{t}{m_\tau^2}\right)^2 \lambda^{1/2}(t, m_-^2, m_0^2) \\ &\times \left[C_V^2 |\tilde{F}_+(t)|^2 \left(1 + \frac{2t}{m_\tau^2}\right) \lambda(t, m_-^2, m_0^2) + 3C_S^2 \Delta_{-0}^2 |\tilde{F}_0(t)|^2 \right] G_{\text{EM}}(t). \end{aligned} \quad (7)$$

Here, the short-distance electroweak corrections are encoded in S_{EM} [47–54], V_{uD} ($D = d, s$) refers to the CKM matrix element and G_F is the Fermi constant.

The $G_{\text{EM}}(t)$ factor includes the QED corrections to the $\tau^- \rightarrow P_1^- P_2^0 \nu_\tau$ with virtual plus real photon radiationⁱⁱⁱ. We split the contributions to $G_{\text{EM}}(t)$ in two parts: $G_{\text{EM}}^{(0)}(t)$, which includes the non-radiative with the virtual contribution plus the leading Low approximation, and $\delta G_{\text{EM}}(t)$, which encodes the remaining contributions to the amplitude. The prediction for both are depicted in Fig. 5, where model 1/2 describe the factorization prescription of the radiative correction to the form factors^{iv}.

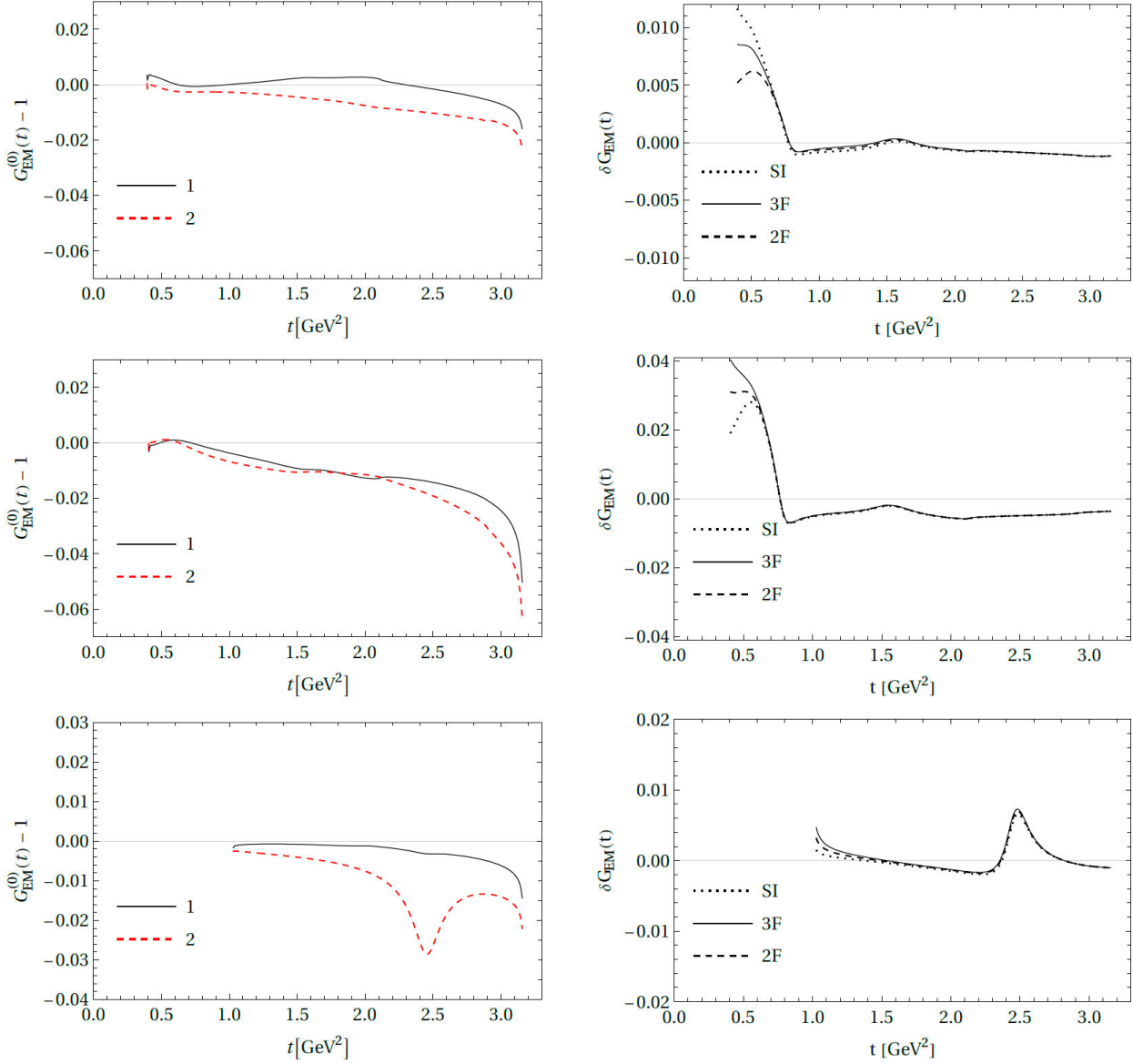


FIGURE 5. Correction factors $G_{EM}^{(0)}(t)$ (left) and $\delta G_{EM}(t)$ (right) to the differential decay rates of the $K^- \pi^0$, $\bar{K}^0 \pi^-$, $K^- K^0$, and $\pi^- \pi^0$ modes from top to bottom.

Integrating upon t , we obtain

$$\Gamma_{PP(\gamma)} = \frac{G_F^2 S_{EW} m_\tau^5}{96\pi^3} |V_{uD} F_+(0)|^2 I_{PP}^\tau (1 + \delta_{EM}^{PP})^2, \quad (8)$$

where

$$I_{PP}^\tau = \frac{1}{8m_\tau^2} \int_{t_{thr}}^{m_\tau^2} \frac{dt}{t^3} \left(1 - \frac{t}{m_\tau^2}\right)^2 \lambda^{1/2}(t, m_-^2, m_0^2) \left[C_V^2 |\tilde{F}_+(t)|^2 \left(1 + \frac{2t}{m_\tau^2}\right) \lambda(t, m_-^2, m_0^2) + 3C_S^2 \Delta_{-0}^2 |\tilde{F}_0(t)|^2 \right]. \quad (9)$$

These results are summarized in Table II. The second column shows a former estimation of the radiative corrections [33] which is in agreement with the results for Model 1 and Model 2 in the third and fourth column, respectively. In Ref. [34], an estimation of the radiative corrections gave $\delta_{EM}^{\bar{K}^0 \pi^-} = \delta_{EM}^{m.i.}/2 \simeq -0.063\%$ which also agrees with our results. The last three columns represent the remaining contribution using $\delta G_{EM}(t)$ in Fig. 5.

The overall contribution is obtained by adding the results from $G_{EM}^{(0)}(t)$ and $\delta G_{EM}(t)$. Using the outcomes from Model 1 and $\delta G_{EM}(t)$ with 3F, we get

TABLE II. Electromagnetic corrections to hadronic τ decays in %.

δ_{EM}	Ref. [33]	$G_{EM}^{(0)}(t)$		$\delta G_{EM}(t)$		
		Model 1	Model 2	SI	SI + 2F	SI + 3F
$K^- \pi^0$	-0.20(20)	-0.019	-0.137	-0.001	+0.006	+0.010
$\bar{K}^0 \pi^-$	-0.15(20)	-0.086	-0.208	-0.098	-0.085	-0.080
$K^- K^0$	-	-0.046	-0.223	-0.012	+0.003	+0.016
$\pi^- \pi^0$	-	-0.196	-0.363	-0.010	-0.002	+0.010

$$\begin{aligned}\delta_{EM}^{K^- \pi^0} &= - (0.009_{-0.118}^{+0.008}) \%, \\ \delta_{EM}^{\bar{K}^0 \pi^-} &= - (0.166_{-0.122}^{+0.010}) \%, \\ \delta_{EM}^{K^- K^0} &= - (0.030_{-0.179}^{+0.026}) \%,\end{aligned}\quad (10)$$

where the main asymmetric uncertainty comes from the difference between model 1 and 2. Additionally, we take the difference between the 2F and 3F results as a symmetric error for our model-dependence.

Finally, we can use the results for the $\pi^- \pi^0$ decay mode in Ref. [29] to get

$$\delta_{EM}^{\pi^- \pi^0} = - (0.186_{-0.169}^{+0.024}) \%, \quad (11)$$

which is in agreement with the value reported in Ref. [32], $\delta_{EM}^{\pi^- \pi^0} \simeq -0.08\%$, using the VMD model for the SD contribution.

5. Conclusions

At the current level of precision achieved in semileptonic tau decays, radiative corrections are required to test the SM and to extract information about NP.

In this work, we investigate the electromagnetic corrections to the hadronic tau decays. Specifically, we present a new calculation of the long-distance radiative corrections to the $\tau^- \rightarrow (P_1 P_2)^- \nu_\tau$ decays for the $K^- \pi^0$, $\bar{K}^0 \pi^-$ and $K^- K^0$ decay modes^v. Although the model-independent contribution of these corrections was already available for the $K\pi$ modes, a survey of the structure-dependent one was missing in the literature. Our results, which align with prior estimates for the $(K\pi)^-$ decay channels, bridge this gap and decrease the uncertainty by a factor approximately 2, enabling more precise tests of NP.

Acknowledgements

I wish to thank the organizers for the pleasant conference. I also would like to thank R. Escribano and P. Roig for their comments on the manuscript. This work has been supported by MICINN with funding from European Union NextGenerationEU (PRTR-C17.I1) and by Generalitat de Catalunya. I acknowledge Conacyt for my PhD scholarship. IFAE is partially funded by the CERCA program of the Generalitat de Catalunya.

- i.* Further details can be found in Ref. [42].
- ii.* The former corresponds to the constraints from up to 3-Green functions which includes operators that contribute at $\mathcal{O}(p^6)$ in $R\chi T$, while the second are the constraints from just 2-Green functions.
- iii.* $G_{EM}(t)$ was originally studied in Ref. [29] using $R\chi T$ at $\mathcal{O}(p^4)$ and recently at $\mathcal{O}(p^6)$ in Ref. [31] for the $\pi^- \pi^0$ decay mode. Additionally, a reevaluation of $G_{EM}(t)$ for these decays was performed in Ref. [30, 32] using a Vector Meson Dominance (VMD) model [55].
- iv.* See Eqs. (4.2)-(4.3) in Ref. [42] for further details.
- v.* Additionally, an estimation of the radiative corrections to the $K^- \eta^{(\prime)}$ modes using only $G_{EM}^{(0)}(t)$ gave $\delta_{EM}^{K^- \eta} = - (0.026_{-0.162}^{+0.024}) \%$ and $\delta_{EM}^{K^- \eta'} = - (0.304_{-0.030}^{+0.380}) \%$ [42].
1. M. Davier, A. Hocker, and Z. Zhang, The Physics of Hadronic Tau Decays, *Rev. Mod. Phys.* **78** (2006) 1043, <https://doi.org/10.1103/RevModPhys.78.1043>.
2. A. Pich, Precision Tau Physics, *Prog. Part. Nucl. Phys.* **75** (2014) 41, <https://doi.org/10.1016/j.pnpnp.2013.11.002>.
3. G. Abbiendi *et al.*, A Study of one prong tau decays with a charged kaon, *Eur. Phys. J. C* **19** (2001) 653, <https://doi.org/10.1007/s100520100632>.
4. S. Schael *et al.*, Branching ratios and spectral functions of tau decays: Final ALEPH measurements and physics implications, *Phys. Rept.* **421** (2005) 191, <https://doi.org/10.1016/j.physrep.2005.06.007>.
5. B. Aubert *et al.*, Measurements of Charged Current Lepton Universality and using Tau Lepton Decays to *Phys. Rev. Lett.* **105** (2010) 051602, <https://doi.org/10.1103/PhysRevLett.105.051602>.
6. K. Ackerstaff *et al.*, Measurement of the strong coupling constant α_s and the vector and axial vector spectral functions in hadronic tau decays, *Eur. Phys. J. C* **7** (1999) 571, <https://doi.org/10.1007/s100529901061>.

7. S. Anderson *et al.*, Hadronic structure in the decay, *Phys. Rev. D* **61** (2000) 112002, <https://doi.org/10.1103/PhysRevD.61.112002>.
8. M. Fujikawa *et al.*, High-Statistics Study of the Decay, *Phys. Rev. D* **78** (2008) 072006, <https://doi.org/10.1103/PhysRevD.78.072006>.
9. J. P. Lees *et al.*, Measurement of the spectral function for the decay, *Phys. Rev. D* **98** (2018) 032010, <https://doi.org/10.1103/PhysRevD.98.032010>.
10. Y. Jin *et al.*, Observation of and search for *Phys. Rev. D* **100** (2019) 071101, <https://doi.org/10.1103/PhysRevD.100.071101>.
11. E. A. Garcés, *et al.*, Effective-field theory analysis of the decays, *JHEP* **12** (2017) 027, [https://doi.org/10.1007/JHEP12\(2017\)027](https://doi.org/10.1007/JHEP12(2017)027).
12. V. Cirigliano, A. Crivellin, and M. Hoferichter, No-go theorem for nonstandard explanations of the CP asymmetry, *Phys. Rev. Lett.* **120** (2018) 141803, <https://doi.org/10.1103/PhysRevLett.120.141803>.
13. J. A. Miranda and P. Roig, Effective-field theory analysis of decays, *JHEP* **11** (2018) 038, [https://doi.org/10.1007/JHEP11\(2018\)038](https://doi.org/10.1007/JHEP11(2018)038).
14. V. Cirigliano, *et al.*, Hadronic τ Decays as New Physics Probes in the LHC Era, *Phys. Rev. Lett.* **122** (2019) 221801, <https://doi.org/10.1103/PhysRevLett.122.221801>.
15. J. Rendón, P. Roig, and G. Toledo Sánchez, Effective-field theory analysis of the decays, *Phys. Rev. D* **99** (2019) 093005, <https://doi.org/10.1103/PhysRevD.99.093005>.
16. F.-Z. Chen, *et al.*, CP asymmetry in decays within the Standard Model and beyond, *Phys. Rev. D* **100** (2019) 113006, <https://doi.org/10.1103/PhysRevD.100.113006>.
17. S. González-Solís, *et al.*, Effective-field theory analysis of the decays, *Phys. Rev. D* **101** (2020) 034010, <https://doi.org/10.1103/PhysRevD.101.034010>.
18. S. González-Solís, *et al.*, Exclusive hadronic tau decays as probes of non-SM interactions, *Phys. Lett. B* **804** (2020) 135371, <https://doi.org/10.1016/j.physletb.2020.135371>.
19. F.-Z. Chen, X.-Q. Li, and Y.-D. Yang, CP asymmetry in the angular distribution of decays, *JHEP* **05** (2020) 151, [https://doi.org/10.1007/JHEP05\(2020\)151](https://doi.org/10.1007/JHEP05(2020)151).
20. M. A. Arroyo-Ureña, *et al.*, One-loop determination of branching ratios and new physics tests, *JHEP* **02** (2022) 173, [https://doi.org/10.1007/JHEP02\(2022\)173](https://doi.org/10.1007/JHEP02(2022)173).
21. M. A. Arroyo-Ureña, *et al.*, Radiative corrections to A reliable new physics test, *Phys. Rev. D* **104** (2021) L091502, <https://doi.org/10.1103/PhysRevD.104.L091502>.
22. F.-Z. Chen, *et al.*, CP asymmetry in the angular distributions of decays. Part II. General effective field theory analysis, *JHEP* **01** (2022) 108, [https://doi.org/10.1007/JHEP01\(2022\)108](https://doi.org/10.1007/JHEP01(2022)108).
23. V. Cirigliano, *et al.*, Semileptonic tau decays beyond the Standard Model, *JHEP* **04** (2022) 152, [https://doi.org/10.1007/JHEP04\(2022\)152](https://doi.org/10.1007/JHEP04(2022)152).
24. Z.-H. Guo and P. Roig, One meson radiative tau decays, *Phys. Rev. D* **82** (2010) 113016, <https://doi.org/10.1103/PhysRevD.82.113016>.
25. A. Guevara, G. López Castro, and P. Roig, Weak radiative pion vertex in decays, *Phys. Rev. D* **88** (2013) 033007, <https://doi.org/10.1103/PhysRevD.88.033007>.
26. A. Guevara, G. L. Castro, and P. Roig, Improved description of dilepton production in decays, *Phys. Rev. D* **105** (2022) 076007, <https://doi.org/10.1103/PhysRevD.105.076007>.
27. Y. Aoki *et al.*, FLAG Review 2021, *Eur. Phys. J. C* **82** (2022) 869, <https://doi.org/10.1140/epjc/s10052-022-10536-1>.
28. V. Cirigliano, G. Ecker, and H. Neufeld, Isospin violation and the magnetic moment of the muon, *Phys. Lett. B* **513** (2001) 361, [https://doi.org/10.1016/S0370-2693\(01\)00764-X](https://doi.org/10.1016/S0370-2693(01)00764-X).
29. V. Cirigliano, G. Ecker, and H. Neufeld, Radiative tau decay and the magnetic moment of the muon, *JHEP* **08** (2002) 002, <https://doi.org/10.1088/1126-6708/2002/08/002>.
30. A. Flores-Tlalpa, *et al.*, Model-dependent radiative corrections to $\tau\to\pi-\pi_0$ revisited, *Nucl. Phys. B Proc. Suppl.* **169** (2007) 250, <https://doi.org/10.1016/j.nuclphysbps.2007.03.011>.
31. J. A. Miranda and P. Roig, New based evaluation of the hadronic contribution to the vacuum polarization piece of the muon anomalous magnetic moment, *Phys. Rev. D* **102** (2020) 114017, <https://doi.org/10.1103/PhysRevD.102.114017>.
32. F. Flores-Baez, *et al.*, Long-distance radiative corrections to the di-pion tau lepton decay, *Phys. Rev. D* **74** (2006) 071301, <https://doi.org/10.1103/PhysRevD.74.071301>.
33. M. Antonelli, *et al.*, Predicting the τ strange branching ratios and implications for V_{us} , *JHEP* **10** (2013) 070, [https://doi.org/10.1007/JHEP10\(2013\)070](https://doi.org/10.1007/JHEP10(2013)070).
34. F. V. Flores-Baéz and J. R. Morones-Ibarra, Model Independent Electromagnetic corrections in hadronic decays, *Phys. Rev. D* **88** (2013) 073009, <https://doi.org/10.1103/PhysRevD.88.073009>.
35. F. E. Low, Bremsstrahlung of very low-energy quanta in elementary particle collisions, *Phys. Rev.* **110** (1958) 974, <https://doi.org/10.1103/PhysRev.110.974>.
36. T. H. Burnett and N. M. Kroll, Extension of the low soft photon theorem, *Phys. Rev. Lett.* **20** (1968) 86, <https://doi.org/10.1103/PhysRevLett.20.86>.
37. A. Guevara, G. López-Castro, and P. Roig, decays as backgrounds in the search for second class currents, *Phys. Rev. D* **95** (2017) 054015, <https://doi.org/10.1103/PhysRevD.95.054015>.
38. G. Ecker, *et al.*, The Role of Resonances in Chiral Perturbation Theory, *Nucl. Phys. B* **321** (1989) 311, [https://doi.org/10.1016/0550-3213\(89\)90346-5](https://doi.org/10.1016/0550-3213(89)90346-5).
39. G. Ecker, *et al.*, Chiral Lagrangians for Massive Spin 1 Fields, *Phys. Lett. B* **223** (1989) 425, [https://doi.org/10.1016/0370-2693\(89\)91627-4](https://doi.org/10.1016/0370-2693(89)91627-4).

40. J. Wess and B. Zumino, Consequences of anomalous Ward identities, *Phys. Lett. B* **37** (1971) 95, [https://doi.org/10.1016/0370-2693\(71\)90582-X](https://doi.org/10.1016/0370-2693(71)90582-X).
41. E. Witten, Global Aspects of Current Algebra, *Nucl. Phys. B* **223** (1983) 422, [https://doi.org/10.1016/0550-3213\(83\)90063-9](https://doi.org/10.1016/0550-3213(83)90063-9).
42. R. Escribano, A. Miranda, and P. Roig, Radiative corrections to the decays (2023)
43. V. Cirigliano, *et al.*, The $\langle VAP \rangle$ Green function in the resonance region, *Phys. Lett. B* **596** (2004) 96, <https://doi.org/10.1016/j.physletb.2004.06.082>.
44. V. Cirigliano, *et al.*, Towards a consistent estimate of the chiral low-energy constants, *Nucl. Phys. B* **753** (2006) 139, <https://doi.org/10.1016/j.nuclphysb.2006.07.010>.
45. K. Kampf and J. Novotny, Resonance saturation in the oddintrinsic parity sector of low-energy QCD, *Phys. Rev. D* **84** (2011) 014036, <https://doi.org/10.1103/PhysRevD.84.014036>.
46. P. Roig and J. J. Sanz Cillero, Consistent high-energy constraints in the anomalous QCD sector, *Phys. Lett. B* **733** (2014) 158, <https://doi.org/10.1016/j.physletb.2014.04.034>.
47. A. Sirlin, Radiative corrections to $GV/G\hat{I}_4^{\frac{1}{2}}$ in simple extensions of the $SU(2) \times U(1)$ gauge model, *Nucl. Phys. B* **71** (1974) 29, [https://doi.org/10.1016/0550-3213\(74\)90254-5](https://doi.org/10.1016/0550-3213(74)90254-5).
48. A. Sirlin, Current Algebra Formulation of Radiative Corrections in Gauge Theories and the Universality of the Weak Interactions, *Rev. Mod. Phys.* **50** (1978) 573, <https://doi.org/10.1103/RevModPhys.50.573>.
49. A. Sirlin, Large m_W , m_Z Behavior of the $O(\alpha)$ Corrections to Semileptonic Processes Mediated by W , *Nucl. Phys. B* **196** (1982) 83, [https://doi.org/10.1016/0550-3213\(82\)90303-0](https://doi.org/10.1016/0550-3213(82)90303-0).
50. W. J. Marciano and A. Sirlin, Radiative Corrections to beta Decay and the Possibility of a Fourth Generation, *Phys. Rev. Lett.* **56** (1986) 22, <https://doi.org/10.1103/PhysRevLett.56.22>.
51. W. J. Marciano and A. Sirlin, Electroweak Radiative Corrections to tau Decay, *Phys. Rev. Lett.* **61** (1988) 1815, <https://doi.org/10.1103/PhysRevLett.61.1815>.
52. W. J. Marciano and A. Sirlin, Radiative corrections to $\pi_{\ell 2}$ decays, *Phys. Rev. Lett.* **71** (1993) 3629, <https://doi.org/10.1103/PhysRevLett.71.3629>.
53. E. Braaten and C.-S. Li, Electroweak radiative corrections to the semihadronic decay rate of the tau lepton, *Phys. Rev. D* **42** (1990) 3888, <https://doi.org/10.1103/PhysRevD.42.3888>.
54. J. Erler, Electroweak radiative corrections to semileptonic tau decays, *Rev. Mex. Fis.* **50** (2004) 200.
55. J. J. Sakurai, Theory of strong interactions, *Annals Phys.* **11** (1960) 1, [https://doi.org/10.1016/0003-4916\(60\)90126-3](https://doi.org/10.1016/0003-4916(60)90126-3).